A study of precipitation and recrystallization behaviour of aluminium alloy AA1235

R. K. ROY
Department of Metallurgical and Materials Engineering, Indian Institute of Technology, Kharagpur 721302, India

S. KAR
Department of Materials Science and Engineering, The Ohio State University, OH 43210, USA

K. DAS, S. DAS
Department of Metallurgical and Materials Engineering, Indian Institute of Technology, Kharagpur 721302, India
E-mail: sdas@metal.iitkgp.ernet.in

Published online: 4 February 2006

The recrystallization behaviour of 92% cold rolled commercial pure aluminium has been studied. Annealing was done at different conditions to evaluate the effect of recrystallization temperature and time on the microstructure and texture of the alloy along with a study of subsequent precipitation. Variation of orientation between grains has been studied by the orientation imaging microscopy (OIM). During precipitation, cube component $\{001\}<100>$ has dropped and rolling texture component $\{112\} < \bar{1}\bar{1}1 >$ has increased comparatively. Recrystallization texture is the combination of cube, rolling and random texture. However, during grain growth strong cube grains have formed. A significant number of dislocations are present during grain growth owing to the pinning effect of Al_3Fe particles.

1. Introduction

It is well known that rapid solidification may result in a supersaturated solid solution [1, 2]. After continuous casting of commercial purity aluminium, iron stays in the supersaturated solid solution of aluminium owing to rapid cooling rate. Upon rolling and subsequent annealing, iron comes out from the solid solution and precipitated as Al_3Fe particles [3]. The mutual interaction of precipitation and recrystallization has been extensively studied by Hornbogen and Köster [4]. Precipitates either enhance or inhibit the process of recrystallization. A large number of publications are available relating to the influence of dispersed particles on the recrystallization kinetics of two-phase alloys [5–11]. Recrystallization phenomenon is largely affected by the events at the particle-matrix interface rather than on changes within the particles themselves. This happens owing to a difference in number of dislocations at the particle-matrix interface than the matrix during deformation process; this results in recrystallized nuclei during annealing [12–14]. It is revealed that particle stimulated nucleation (PSN) happens at the deformation zone of the particle-matrix interface when critical particle size is greater than 1 μm [15]. Fine particles (less than 0.1 μm in diameter) retard the start of recrystallization by promoting a homogeneous distribution of dislocations. Vatne *et al*. [16] discussed these two effects of particles on recrystallization textures and microstructures at length. Cube nuclei prevail in a heavily deformed material when a significant amount of dispersoids are present prior to annealing as well as when precipitation occurs during the early stage of annealing. This is dependent on a combination of factors including nucleus size, reduced internal subgrain boundary energy and possibly reduced energy of cube band boundaries [17]. Some researchers [18] observed a decrease in cube texture with the presence of dispersoids. Conversely, the formation of cube texture is also enhanced during precipitation which occurs concurrently with recrystallization [19]. Therefore, the development of texture during recrystallization is quite complicated due to the presence of particles. Generally commercial Al alloys contain three types of recrystallization texture-cube texture, the retained rolling texture and the random texture [20–23]. The warm, extruded commercial purity aluminium shows 40–75% near-cube grains (within 20°

0022-2461
DOI: 10.1007/s10853-005-2226-y

of cube) frequency, compared to 4% frequency expected for random nucleation [24]. However, cold rolled commercially pure aluminium shows a significant balance between cube orientation and random orientation after complete recrystallization [22].

In the present study the precipitation and recrystallization behaviour of 92% cold rolled aluminium alloy AA1235 have been reported at different annealing conditions.

2. Experimental details

The alloy chosen for this research work is a commercially pure aluminium alloy (AA1235), which contains 0.67Fe, 0.16Si, 0.01 Ti and balance Al (all in wt%). This alloy was cold rolled by 92% from a continuously cast slab by multistep cold rolling. The cold rolled alloy was recrystallized at different temperatures with the variation of annealing time to study the change of microstructure and texture.

Recrystallization and subsequent precipitation reaction were jointly studied by the differential scanning calorimetry (DSC). The DSC measurements were performed using a Perkin-Elmer Diamond DSC instrument controlled by the Pyris software. Runs were carried out at the heating rate of 10°C/min. Recrystallization peak observed in DSC thermogram was complemented by microhardness measurement using a Leica VMHT micro-hardness tester at a load of 10 g for 20 s. Subsequent precipitation peak in DSC thermogram was confirmed by a four-probe resistivity measurement method using Keithley nano-voltmeter (2182) and source meter (2400).

For the preparation of thin foils of transmission electron microscopy (TEM) study, sample of 10 × 10 mm dimension was cut from 0.55 mm thick aluminium sheet. Thereafter, it was mounted on a jig using thermoplastic wax and it was thinned down to 80–100 μm thickness by grinding on a 600 grit SiC paper at a low speed (70 rpm) wheel under flowing water. After reaching specified thickness sample was taken out from the jig by applying acetone and 3 mm discs were punched out using a high precision punching machine. Discs were jet-polished using a Struers Tenupol 5 unit in an electrolyte consisting of 70% methanol and 30% concentrate nitric acid at a temperature maintained between −30 and −20°C. Immediately after jet polishing, samples were stored inside a vacuum chamber and studied in a Philips CM12 TEM operating at 120 KV. Orientation imaging microscopy (OIM) was performed on mirror polished longitudinal sections of specimens in the various annealed conditions. At least two different surfaces of each sample were scanned during OIM on the total minimum area of 400 μm by 400 μm. Orientation data were analyzed by the software package TSL (Tex-scan Ltd.)

3. Results and discussion

3.1. Interaction between precipitation and recrystallization

During annealing of commercial alloys, the presence of the alloying element in solid solution or as precipitates is one of the important factors for controlling the microstructure and texture of alloys. Differential scanning calorimeter (DSC) is a good instrument to study the sequence of precipitation and recrystallization. In DSC thermogram, exothermal peak represents recovery, recrystallization and precipitation where as endothermal peak is for the dissolution of phases. In Fig. 1, the first exothermal peak (A) is perhaps related to both recovery and precipitation. Although, this correlation is not quite a straightforward one; still a maximum decrease in electrical resistivity around 300°C suggests a precipitation reaction at that stage (Fig. 2). The main exothermal peak (B) is due to recrystallization. To confirm the recrystallization peak, Vickers microhardness measurements were done on the samples taken out from the DSC instrument after heating to the required temperature followed by an immediate cooling (120°C/min); the results of which are also shown in Fig. 1. The sudden drop of microhardness value coincides with the temperature range of recrystallization

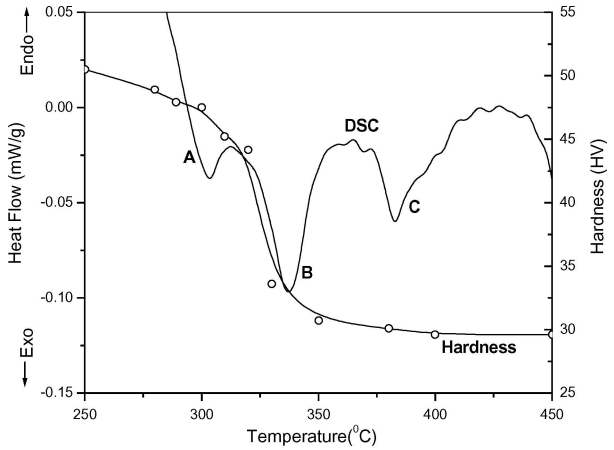

Figure 1 DSC curve for AA1235 alloy 92% cold rolled at the heating rate of 10°C/min. Measurements of vickers hardness during DSC run carried out at room temperature on samples taken out of the DSC apparatus.

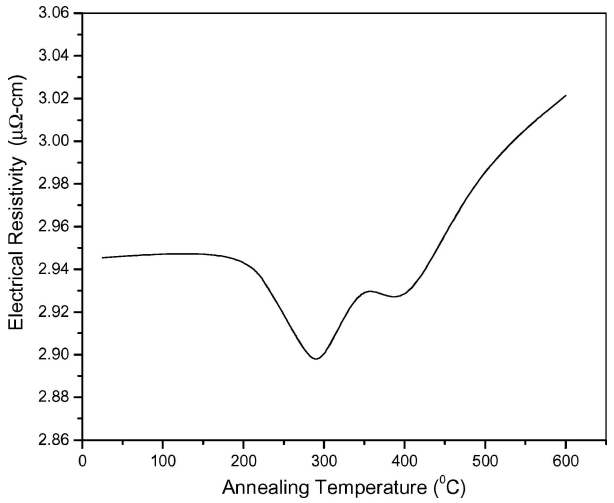

Figure 2 Change of resistivity of 92% cold rolled AA1235 alloy as a function of temperatures for 60 min annealing.

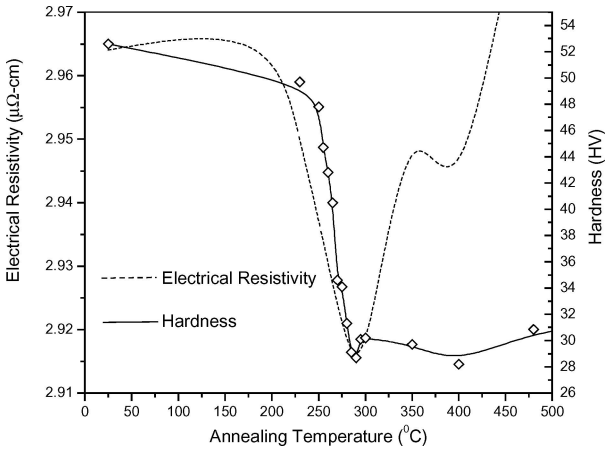

Figure 3 Microhardness and electrical resistivity of the cold rolled alloy as a function of temperature after 60 min of isothermal annealing [25].

peak in DSC thermogram. Recrystallization completes at around 360°C and subsequently the precipitation reaction starts, which is clearly explained by the third exothermal peak at C.

Fig. 2 shows the variation of electrical resistivity as a function of annealing temperature. It is shown that no change in electrical resistivity up to 200°C, and then it continuously decreases to its lowest value at 300°C. The maximum decrease in electrical resistivity around 300°C suggests a precipitation reaction at that stage (Fig. 2). At 400°C, a small hump in resistivity curve may be for precipitation. It is evident from DSC thermogram obtained during linear heating and electrical resistivity that precipitation takes place mostly prior to recrystallization. However, present researchers have also observed the evidence of precipitation and recrystallization taking place simultaneously during isothermal heating [25]. Fig. 3 shows a sudden drop of hardness due to recrystallization and lowering of electrical resistivity due to precipitation at the same temperature range during isothermal heating of the alloy. The linear heating in DSC delays the rearrangement of dislocations hence the recrystallization, where as the isothermal heating helps in providing sufficient time for the rearrangement of dislocations resulting in simultaneous occurrence of precipitation and recrystallization. Therefore, it is likely that the precipitation of Al_3Fe particles takes place simultaneously with recrystallization during isothermal heating and prior to and after recrystallization during linear heating in a DSC.

3.2. Recrystallized microstructure

Recrystallized microstructures and precipitates are observed by transmission electron microscopy (TEM). The alloy shows dislocation networks with fine precipitates of average size of 0.2 μm in the as-rolled condition (Fig. 4a). Figs. 4b and c show subgrain structure formation by the reorientation of dislocations to create the stable low angle boundaries and subsequent precipitation of fine (0.5 μm) Al_3Fe particles after annealing at 250°C for 240 min. During annealing of supersaturated alloys, substructure is a favoured site for precipitation. Particles are easily nucleated at the sub-boundaries due to fast diffusion paths near the boundaries [16]. Fine particles precipitated at sub-boundary inhibit the boundary migration during primary recrystallization (Fig. 4c). At high temperature (480°C), dissolution of particles takes place and this leads to the grain growth at high temperature (Fig. 4d). At this stage a pinning effect of remaining large Al_3Fe precipitates is responsible for the presence of a significant number of dislocations even at full annealed condition (Fig. 4e).

3.3. Orientation imaging microscopy (OIM)

Inverse Pole figure (IPF) maps of different grains have been obtained by OIM as shown in Fig. 5. In the OIM technique, orientation of each grain is detected by electron back scattered diffraction pattern (EBSDP). The colour/gray scale of the grains is related to crystal axis aligning with the sample normal direction. The same colour/gray scale grains have same crystal orientation. The colour/gray scale change indicates a significant orientation gradient developed during recrystallization of the material. Upon annealing, three types of orientations (cube, rolling and random) are observed here. Computational software was used to measure the size and number of grains of different orientation from the IPF maps and calculation of volume fraction of different texture components [22].

Fig. 5a shows orientation of the grains at an early stage of recrystallization. It is seen that initially a higher fraction of cube-oriented grains recrystallizes and grows from a cube band and from prior grain boundaries. Due to the presence of small size particles there was no evidence of nucleation at particles. Higginsion et al. have also found the same type of nucleation behaviour in Al-Mn-Si alloys [17]. Small particles retard both the nucleation and growth of recrystallized grains. For viable nuclei formation, it should reach the critical size. The cube subgrains may easily reach the critical value due to large initial cube subgrain size and the high recovery rate during the initial recovery period before the onset of precipitation [16]. Thus the nucleation from cube bands is not strongly affected by the precipitation reaction. Initially grains with cube orientation dominate over other orientations. However, with an increase in annealing time cube grains generally grow very slowly owing to the effect of solute drag and/or precipitation; this accounts for the development of the rolling component and reduction of the strength of the cube component [26].

At high temperature, a preferred growth of cube-oriented grains gives it the dominance in recrystallization texture. However, it is strongly dependent on the presence of precipitates in the matrix. At 380°C, R-oriented (orientations close to those obtained in the former rolling texture) and randomly oriented grains prevail with an increase in annealing time owing to the hindrance of the growth of cube-oriented grains by precipitates (Fig. 5b).

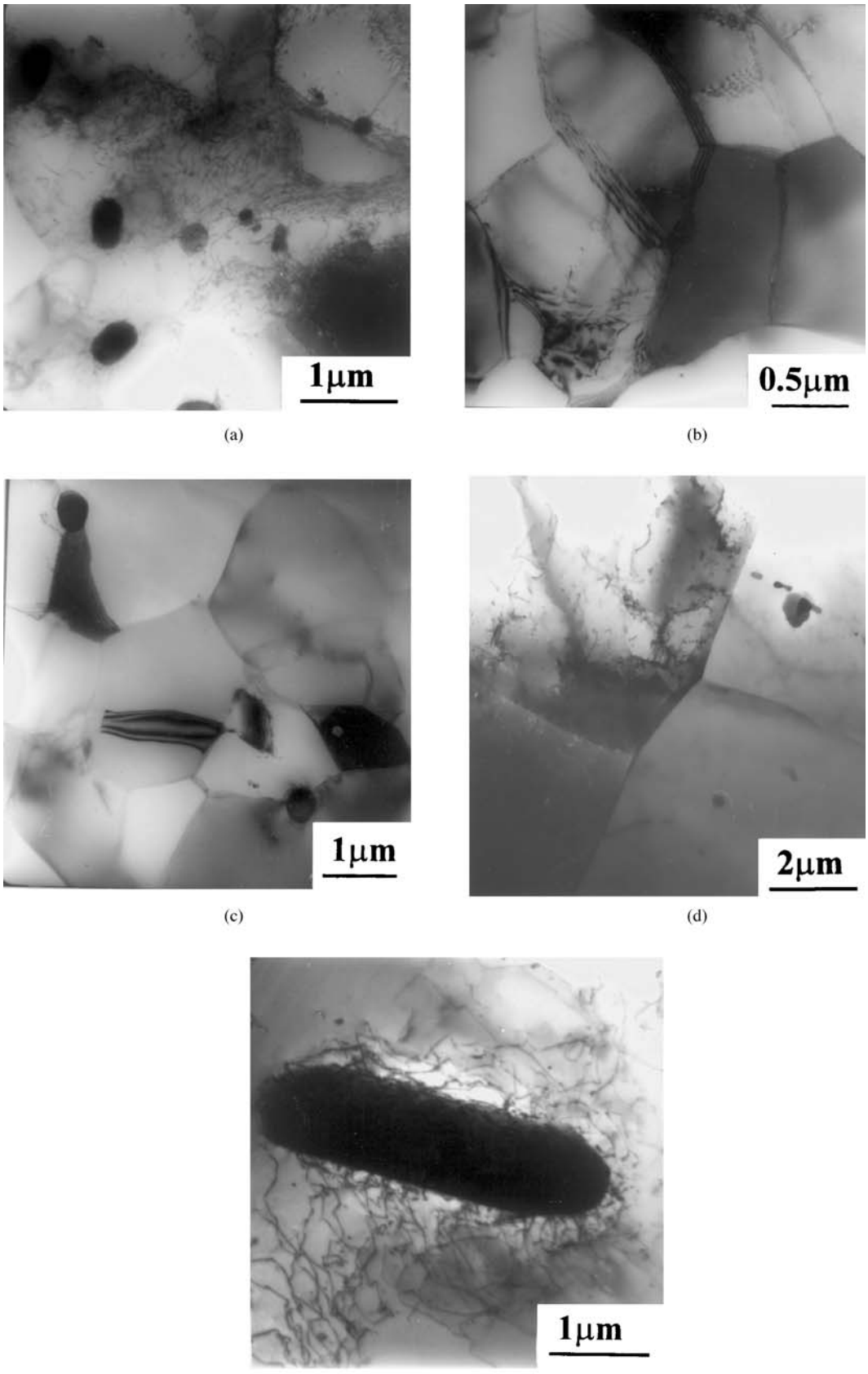

Figure 4 Transmission electron microscopy of the alloy AA1235 (a) as cold rolled and at different annealed conditions (b) and (c) at 250°C for 240 min, (d) and (e) at 480°C for 480 min.

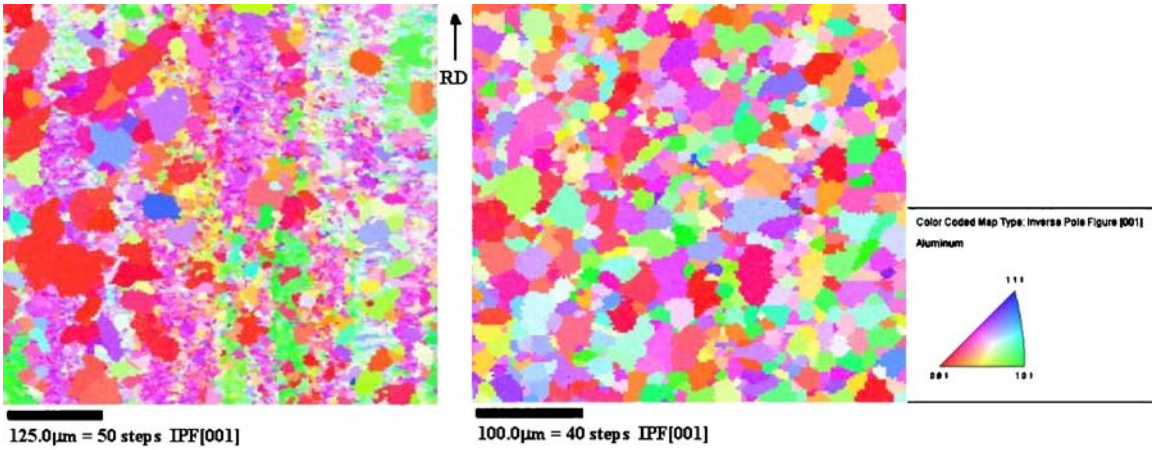

Figure 5 Inverse Pole Figure (IPF) maps obtained by OIM: annealed at (a) 280°C for 30 min, (b) 380°C for 480 min. The rolling direction (RD) is indicated. IPF map shows the direction of crystal axis aligned with the sample normal.

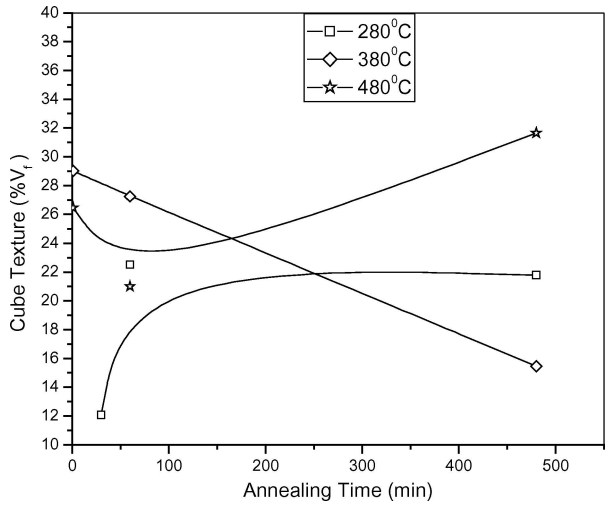

Figure 6 Volume fractions of the cube component as a function of annealing time at different temperatures.

At low temperature, a small amount of precipitates and at high temperature dissolution of some precipitates affect the boundary migration less drastically.

The volume fraction of cube component as a function of annealing time at different temperatures shows that the orientation of grains has continuously changed during recrystallization process (Fig. 6). At 280°C, volume fraction of cube oriented grains initially increases and then becomes constant with annealing time, and at 480°C volume fraction of cube grains has continuously increased with annealing time. However, at 380°C, the volume fraction of cube component has continuously decreased with annealing time.

3.4. Distribution of grains of different orientations

Fig. 7 shows the distribution of grain sizes of different orientations at 380 and 480°C after annealing for 480 min. This distribution is generally between 10–60 μm with the average grain size of 24 and 26 μm for annealing at 380 and 480°C, respectively. It is seen that annealing temperature has no significant effect on the grain size distribution. Recrystallized grains of all the three orientations are inhomogeneously distributed throughout the microstructure. Although, the average grain size of cube oriented grains is larger than the rest, randomly oriented grains are more in number than other two orientations in both annealed conditions. Grain growth as well as recrystallization texture are greatly affected by subsequent precipitation in the alloy. The inhomogeneous distribution of grains can be explained by distribution of precipitated particles. The growth of some grains is completely stopped by the precipitates compared to other grains. It results in the co-existence of large and small grains after complete recrystallization.

3.5. Pole figures

The deformation texture and recrystallization induced [001] texture in the 92% cold rolled aluminium alloy AA1235 was studied by pole figures obtained from the grain orientation data collected by OIM. Fig. 8 shows pole figures as cold rolled and at different annealed conditions. The center of the pole figures corresponds to the normal direction (ND) of specimen surface, which is denoted by [001]. After cold rolling to 92% reduction in thickness, the alloy AA1235 shows rolling texture, $\{112\} < \bar{1}\bar{1}1 >$ (Fig. 8a). During annealing, recrystallization texture develops containing mainly the cube texture component, $\{001\}<100>$, along with the rolling texture component and a relatively large volume fraction of random texture components. During early stage of annealing, small particles may significantly alter the texture evolution owing to the possible influence on nucleation and growth of recrystallized grains [16]. After annealing at 280°C for 60 min, weak cube texture prevails along with some rolling texture (Fig. 8b). Same thing occurs with an increase in annealing time to 480 min (Fig. 8c). However, the rolling texture

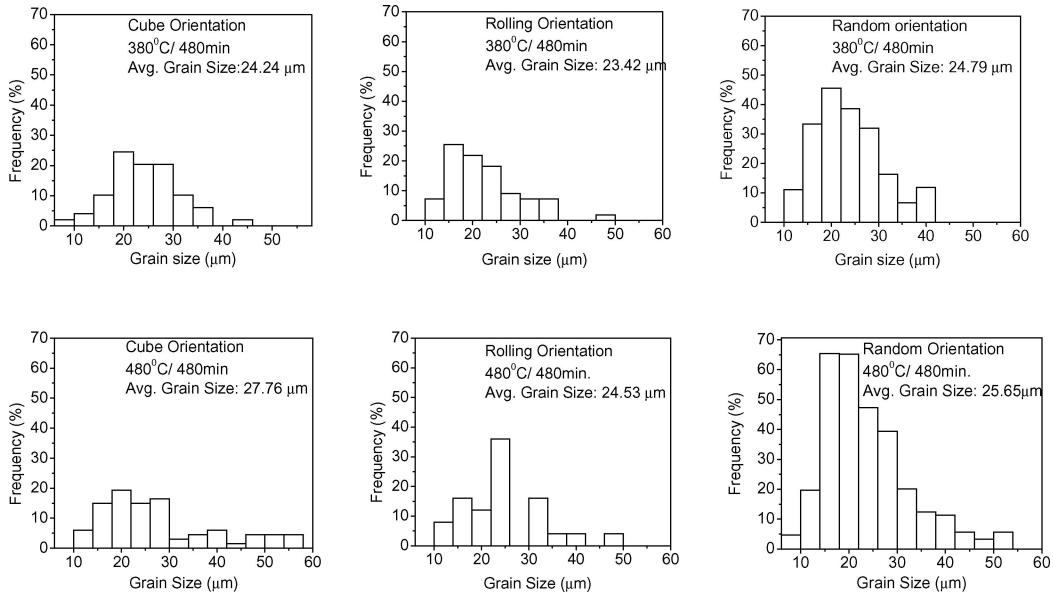

Figure 7 Distribution of grain sizes.

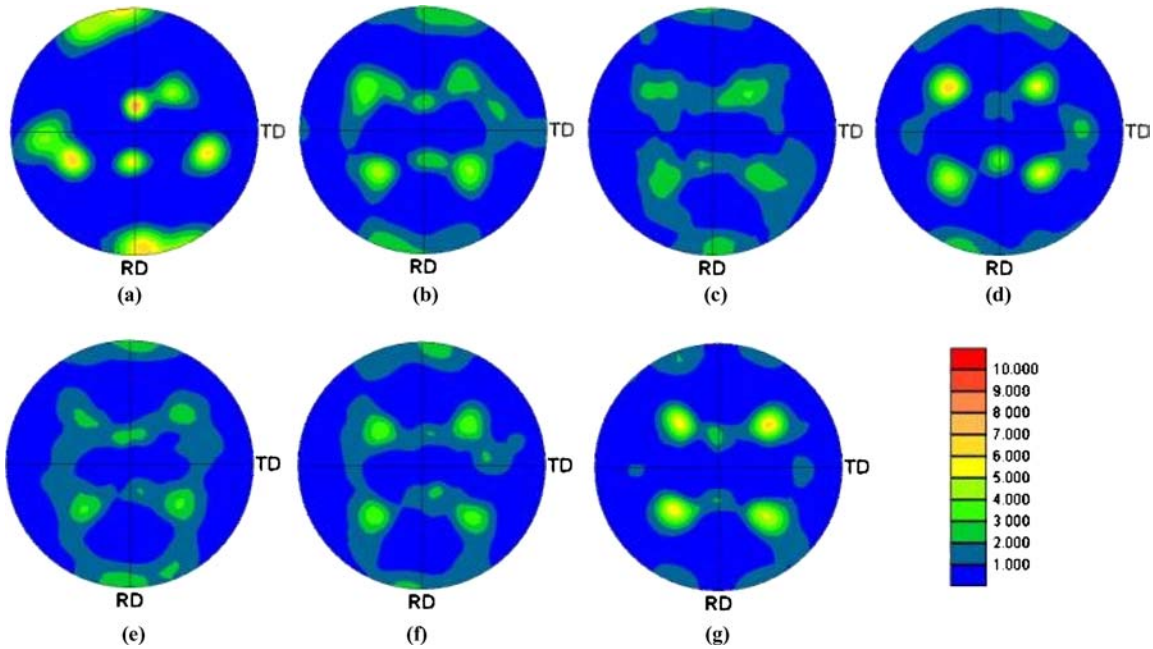

Figure 8 {111} pole figures for the specimen (a) as 92% cold rolled and annealed at (b) 280°C for 60 min, (c) 280°C for 480 min, (d) 380°C for 1 min (e) 380°C for 480 min (f) 480°C for 1 min (g) 480°C for 480 min RD denotes Rolling direction. TD denotes Transverse direction.

continuously disappears with the formation of a random texture. With an increase in temperature to 380°C, just after 1 min of annealing a strong cube texture develops (Fig. 8d). After 480 min of annealing at 380°C, a weak cube texture develops along with a rolling texture owing to a favoured nucleation of the latter (Fig. 8e). Annealing at 480°C for 1 min also favours a weak cube texture (Fig. 8f) and with an increase in annealing time, the cube texture becomes strong (Fig. 8g). However, stronger cube texture develops at 480°C owing to the presence of large precipitates compared to a weak cube texture at 280°C where fine precipitates are present. There has been a general observation that the strength of the cube texture in the fcc alloys has increased during grain growth [27]. It is desirable to achieve an optimum balance between the cube and other texture components to minimize the overall anisotropy.

4. Conclusion

The following conclusions are drawn from the study of precipitation and recrystallization behaviour of 92% cold rolled aluminium alloy AA1235 annealed at different temperatures for different time:

(1) Precipitation reaction takes place at 300 and 400°C.

(2) Precipitation takes place concurrently with the recrystallization during isothermal heating and prior to and after recrystallization during linear heating in a DSC.

(3) Upon annealing, the migration of low and high angle grain boundaries is inhibited by the pinning effect of precipitates.

(4) Due to the hindrance effect of Al_3Fe, a significant number of dislocations is evident even after the completion of recrystallization.

(5) Long annealing time at low (280°C) and intermediate temperatures (380°C), and a short annealing time at high temperature (480°C) enhance the precipitation reaction, which results in a higher volume fraction of rolling and other oriented grains due to the retardation growth of cube oriented grains by the pinning effect of Al_3Fe precipitates.

(6) There is a coexistence of large and small recrystallized grains of all orientations due to the effect of fine precipitates.

(7) The recrystallization texture of 92% cold rolled alloy AA1235 consists of cube texture along with rolling and random textures.

Acknowledgments

Authors wish to acknowledge Prof. H. L. Fraser of the Ohio State University for kindly providing the OIM facility for this research. Financial support received from the Department of Science and Technology, Ministry of Science and Technology, Government of India, New Delhi, to carry out this research is gratefully acknowledged.

References

1. G. FALKENHAGEN and W. HOFMANN, *Z. Metallk.* **43** (1952) 69.
2. P. ESSLINGER, *ibid.*. **57** (1966) 109.
3. J. H. RYU and D. N. LEE, *Mat. Sci. Engg. A* **336** (2002) 225.
4. E. HORNBOGEN, U. KÖSTER, in "Recrystallization of Metallic Materials", edited by F. Haessner (Dr. Riederer Verlag GmbH, Stuttgart, 1978) p. 159.
5. F. J. HUMPHREYS and J. W. MARTIN, *Acta Metall.* **14** (1966) 775.
6. D. T. GAWNE and G. T. HIGGINS, *J. Mater. Sci.* **6** (1971) 403.
7. C. W. CORTI, Ph. D. Thesis, University of Surrey, 1973.
8. J. L. BRIMHALL, M. J. KLEIN and R. A. HUGGINS, *Acta Metall.* **14** (1966) 459.
9. F. J. HUMPHREYS and J. W. MARTIN, *Phil. Mag.* **17** (1968) 365.
10. T. C. ROLLASON and J. W. MARTIN, *Acta Metall.* **18** (1970) 1267.
11. T. GLADMAN, I. D MCIVER and F. B. PICKERING, *J. Iron Steel Inst.*, London, **209** (1971) 380.
12. R. D. DOHERTY and J. W. MARTIN, *J. Inst. Met.* **91** (1963) 332.
13. F. J. HUMPHREYS, *Met. Sci.* **31** (1979) 136.
14. N. HANSEN and B. BAY, *J. Mat. Sci.* **7** (1972) 1351.
15. F. J. HUMPHREYS, *Acta Meall.* **25** (1977) 1323.
16. H. E. VATNE, S. BENUM, O. DAALAND and E. NES, *Text. Microstruct.* **26/27** (1996) 385.
17. R. L. HIGGINSON, M. AINDOW and P. S. BATE, *Mat. Sci. Engg. A* **225** (1997) 9.
18. F. J. HUMPHREYS and D. JUUL JENSEN, in Proceedings of the 7th Riso International Symposium, Riso, Denmark, edited by N. Hansen *et al*., (1986) p. 93.
19. H. E. VATNE, O. ENGLER and E. NES, *Mater. Sci. Forum* **157–162** (1994) 1501.
20. O. ENGLER, J. HIRSCH and K. LÜCKE, *ibid.* **43** (1995) 121.
21. J. HJELEN, R. ØRSUND and E. NES, *Acta Metall. Mater.* **39** (1991) 1377.
22. D. JUUL JENSEN, N. HANSEN and F. J. HUMPHREYS, *Acta Metall.* **33** (1985) 2155.
23. K. LÜCKE and O. ENGLER, in Proceedings of the 3rd International Conference on Al-alloys (ICAA 3), The Norwegian Inst. of Tech., Trondheim, 1992, Vol. III, edited by L. Arnberg *et al*., p. 439.
24. R. D. DOHERTY, K. KASHYAP and S. PANCHANADEESWARAN, *Acta Metall. Mater.* **41** (1993) 3029.
25. R. K. ROY and S. DAS, Unpublished Paper (2004).
26. F. J. HUMPHREYS and M. HATHERLY, in "Recrystallization and Related Annealing Phenomena" (1995) p. 347.
27. W. B. HUTCHINSON and E. NES, in "Grain Growth in Polycrystalline Materials", edited by Abbruzzese and Brozzo (Trans Tech Publns., Rome, 1992) p. 385.

Received 30 November 2004
and accepted 13 May 2005